PCCP

ROYAL SOCIETY OF CHEMISTRY

PAPER

View Article Online
View Journal | View Issue

Cite this: *Phys. Chem. Chem. Phys.*, 2020, **22**, 6176

The valence and Rydberg states of dienes†

Jiaxin Ning and Donald G. Truhlar *

The molecules 1,4-cyclohexadiene (unconjugated 1,4-CHD) and 1,3-cyclohexadiene (conjugated 1,3-CHD) both have two double bonds, but these bonds interact in different ways. These molecules have long served as examples of through-bond and through-space interactions, respectively, and their electronic structures have been studied in detail both experimentally and theoretically, with the experimental assignments being especially complete. The existence of Rydberg states interspersed with the valence states makes the quantum mechanical calculation of their spectra a challenging task. In this work, we explore the electronic excitation energies of 1,4-CHD and 1,3-CHD for both valence and Rydberg states by means of complete active space second-order perturbation theory (CASPT2), extended multi-state CASPT2 (XMS-CASPT2), and multiconfiguration pair-density functional theory (MC-PDFT); it is shown by comparison to experiment that MC-PDFT yields the most accurate results. We found that the inclusion of Rydberg orbitals in the active space not only enables the calculation of Rydberg excitation energies but also improves the accuracy of the valence ones. A special characteristic of the present analysis is the calculation of the second moments of the excited-state orbitals. Because we find that the CASPT2 densities agree well with the CASSCF ones and since the MC-PDFT methods gets accurate excitation energies based on the CASSCF densities, we believe that we can trust these moments as far as giving a more accurate picture of the diffuseness of the excited-state orbitals in these prototype molecules than has previously been available.

Received 24th December 2019,
Accepted 20th February 2020

DOI: 10.1039/c9cp06952f

rsc.li/pccp

1. Introduction

Polychromophoric assemblies are widespread in both biological systems and functional materials, and the 1,4-cyclohexadiene molecule (1,4-CHD) and 1,3-cyclohexadiene molecule (1,3-CHD) are good prototypes for investigating the electronic structures of molecules with interacting double bonds.[1–8] In addition to the structural data, a better understanding of the spectra can be important for interpreting the photo-induced dynamical processes that have been extensively studied.[9] The skeletal formulas of 1,4-CHD and 1,3-CHD are shown in Scheme 1.

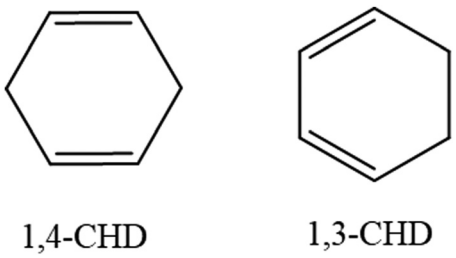

Scheme 1 1,4-CHD and 1,3-CHD molecules. (Hydrogen atoms are not shown.)

In 1,4-CHD, the double bonds are unconjugated, and the four π orbitals interact through the σ orbitals of methylene groups. The consequence is that the out-of-phase combination of the π and π* orbitals has lower energy than the in-phase combination of these orbitals.[10–15] Therefore, the ordering of the four valence π molecular orbitals (MOs) is as follows: HOMO−1 is π–π, HOMO is π+π, LUMO is π*–π*, and LUMO+1 is π*+π*. The excitations involving these MOs have been studied by both experiment[16,17] and quantum mechanical calculation.[15] Electron impact experiments show that some Rydberg states have lower energies than the second valence π* states, as shown in Fig. 1.[16,17] Complete-active-space second-order perturbation theory (CASPT2) calculations by Merchán *et al.* agree with the experimental conclusion that the valence and Rydberg states are interspersed in 1,4-CHD.[15]

In 1,3-CHD, the double bonds are conjugated, and the valence π and π* MOs are ordered in the usual way: HOMO−1 is π + π, HOMO is π − π, LUMO is π* + π*, and LUMO+1 is π* − π*. The excited states of 1,3-CHD have been investigated by various experiments, including electron impact spectroscopy[18,19] and optical spectroscopy.[20,21] The results demonstrate that 1,3-CHD

Department of Chemistry, Chemical Theory Center, and Minnesota Supercomputing Institute, University of Minnesota, Minneapolis, Minnesota 55455, USA.
E-mail: truhlar@umn.edu

† Electronic supplementary information (ESI) available: It contains geometries, active orbitals, and CI vectors. See DOI: 10.1039/c9cp06952f

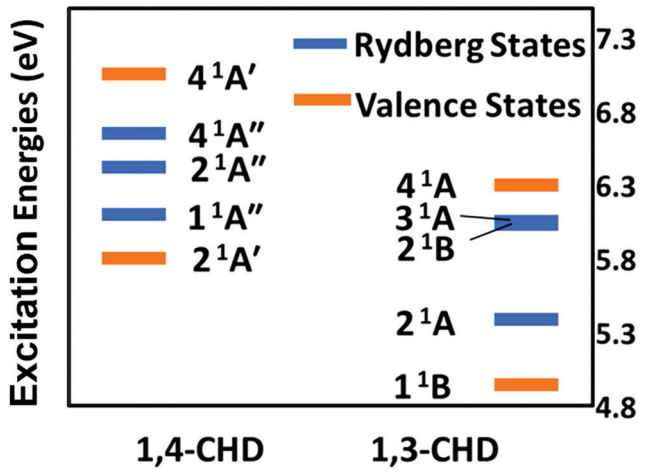

Fig. 1 The experimental excitation energies for 1,4-CHD and 1,3-CHD. 1,4-CHD has C_s symmetry, and 1,3-CHD has C_2 symmetry. Orange and blue lines represent valence and Rydberg excited states, respectively. No experimental data are available for the $3^1A'$ and $3^1A''$ states of 1,4-CHD and the 3^1B state of 1,3-CHD.

also has some Rydberg excited states between the first and the second valence excited states, as shown in Fig. 1.

Various electronic structure calculations of the excited states of 1,3-CHD have been carried out.[21–31] In 2005, Tamura *et al.* reported multi-configuration quasi-degenerate perturbation theory (MCQDPT) calculation with an active space composed of six electrons in four valence π orbitals and two valence σ orbitals and used the 6-31G(d,p) basis set.[32] In 2015, Pemberton *et al.* reported 3-state state-averaged complete active space self-consistent-field calculations (SA(3)-CASSCF(6,4)) with only three valence π orbitals and one occupied σ orbital included in the active space and with the cc-pVDZ basis set, where (n_e,n_o) denotes n_e active electrons in n_o active orbitals.[33] In 2016, Lei *et al.* reported CASSCF(14,8) and CASPT2 calculations with the active space composed of five occupied valence σ orbitals and three valence π orbitals and with the 6-31G* basis set.[34] In 2019, Polyak *et al.* used extended multi-state CASPT2 (XMS-CASPT2) with the same active space that Hiroyuki *et al.* used and with the cc-pVDZ basis set.[35]

An important question tested in the present work is whether the active spaces used in the previous work have diffuse enough orbitals to give a correct description of Rydberg character of all the excited states. We will show that they do not, which is consistent with previous work by Dong and two of the authors, where we showed, in what was called the Goldilocks principle, that basis sets with intermediate diffuseness are needed to calculate consistent excitation energies of π systems.[36]

Quantum mechanical calculations of electronic excitation energies can be carried out by a wide variety of methods, but because of near-degeneracy effects in electronically excited states, we only make calculations here with methods based on SA(n)-CASSCF reference wave functions, because of that method's potential for providing a balanced treatment of strongly coupled states.[37] And we consider three post-SCF methods that start with a SA(n)-CASSCF reference wave function, namely CASPT2,[38–42] XMS-CASPT2,[43,44] and multiconfiguration pair-density functional theory (MC-PDFT).[45] We study the ability of these methods to provide accurate results for the vertical excitation energies for both 1,4-CHD and 1,3-CHD, which are especially interesting because they have states with different amounts of Rydberg character. We explore the dependence of the results on the choice of active space, and we explain why the excitation energies become more accurate when the active spaces include enough Rydberg orbitals.

2. Theory and computational details

All the calculations are performed using the maug-cc-pVTZ basis set[46–48] in the *OpenMolcas 8.3* software package.[49,50] All calculated excitation energies are singlet-to-singlet vertical excitation energies.

For 1,4-CHD, the ground-state geometry is optimized using Kohn–Sham density functional theory[51] with D_{2h} symmetry and with the M06-2X[52] exchange–correlation functional, and all excited-state calculations are carried out enforcing C_s symmetry. For 1,3-CHD, the ground-state geometry is taken from ref. 53, which shows that the molecule has C_2 symmetry, and all the calculations carried out here are conducted using C_2 symmetry. The Cartesian coordinates of the two molecules are given in Tables S1 and S2 (Tables and figures with a prefix S are in the ESI†).

When the symmetry of the excited states is the same as the symmetry of the ground state (A′ for 1,4-CHD; A for 1,3-CHD), the reference wave functions for all the states are obtained by SA(n)-CASSCF(n_e,n_o), and we use the shorthand notation X(n)-(n_e,n_o), where X denotes the irreducible representation (X = A′ or A″ for 1,4-CHD; X = A or B for 1,3-CHD). When the symmetry of the ground state is different from that of excited states, the reference wave function for the ground state is obtained by state-specific CASSCF (SS-CASSCF), denoted as X-SS-(n_e,n_o), and the reference wave functions for the excited states are still obtained by state-averaged calculations. The CASSCF calculations resulting from these choices are specified in the next two paragraphs.

For 1,4-CHD, the CASSCF calculations performed are:

- A′(3)-(4,4): four electrons in four valence π orbitals.
- A′(6)-(4,6): four electrons in four valence π and two Rydberg orbitals.
- A″(6)-(4,8): four electrons in four valence π and four Rydberg orbitals.
- A′-SS-(4,8): four electrons in four valence π and four Rydberg orbitals.

For 1,3-CHD, the CASSCF calculations performed are:

- A-SS-(4,4) and B-SS-(4,4): four electrons in four valence π orbitals.
- A(2)-(4,4): four electrons in four valence π orbitals.
- A(6)-(4,12) and B(6)-(4,12): four electrons in four valence π orbitals and six Rydberg orbitals.
- A-SS-(4,12): four electrons in four valence π orbitals and six Rydberg orbitals.

For 1,4-CHD, the (4,4) active space is referred to as the π-only active space for convenience in the later discussion since it only contains valence π orbitals, and the (4,6) and (4,8) active spaces are referred to as π-plus active spaces since they contain valence

π orbitals plus Rydberg orbitals. Similarly, for 1,3-CHD, (4,4) and (4,12) active spaces are referred to as the π-only and π-plus active spaces, respectively.

A default value of 0.25 E_h is used for the ionization potential-electron affinity (IPEA) shift[54] for all the CASPT2 and XMS-CASPT2 calculations. When calculating 1,3-CHD, a 0.5 E_h real level shift[55,56] is used to avoid possible intruder states.

For MC-PDFT, two on-top functionals are used: translated Perdew–Burke–Ernzerhof (PBE)[45,57] and fully translated PBE,[57,58] labeled as tPBE and ftPBE, respectively.

In the next section, we evaluate the accuracies of the various kinds of calculations by computing the mean unsigned error (MUE) relative to experimental values.

We know from previous work that the second moment can serve to quantify the Rydberg character of states because the greater the second moment for a state (orbital) is, the more Rydberg character this state (orbital) has.[36,59] Thus, we calculate the second moments $\langle x^2\rangle$, $\langle y^2\rangle$, $\langle z^2\rangle$, and $\langle r^2\rangle$ for selected orbitals and states, where

$$\langle r^2\rangle = \langle x^2\rangle + \langle y^2\rangle + \langle z^2\rangle.$$

We use the convention that the second moments include only the contribution of electrons (not nuclei) and are positive numbers (even though the electron density formally has a negative charge). To make it easier to compare the $\langle r^2\rangle$ values of the states, we consider the relative second moment, which is defined as

$$\Delta\langle r^2\rangle = \langle r^2\rangle_{\text{excited state}} - \langle r^2\rangle_{\text{ground state}},$$

where the ground-state $\langle r^2\rangle$ is obtained by the SS calculation.

3. Results and discussion

3.1. Excitation energies of 1,4-CHD

The excitation energies obtained by CASSCF, CASPT2, XMS-CASPT2, and MC-PDFT calculations for 1,4-CHD are summarized in Table 1.

First, we consider the valence states. Table 1 shows that whether using the π-only or the π-plus active space, MC-PDFT always gives the better excitation energies than CASSCF and the more expensive CASPT2 and XMS-CASPT2 for the two valence excited states, $2^1A'$ state and $4^1A'$ state.

By comparing the results obtained using the π-only and π-plus active spaces, we learn whether the inclusion of Rydberg orbitals in the active space has a significant effect on the calculated valence excitation energies. Table 1 shows that when the π-plus active space is used, the MC-PDFT results for valence states become more accurate. Especially notable is that – when the active space changes to π-plus from π-only – the MUE for valence states obtained by ftPBE is decreased to only 0.10 eV from 0.74 eV and the MUE obtained by tPBE is decreased to 0.15 eV from 0.75 eV. Thus, we conclude that active space should include Rydberg orbitals to give more accurate valence excitation energies.

Furthermore, when the π-plus active space is used, the Rydberg excitation energies can also be calculated. Table 1 shows that only MC-PDFT gives the correct energy ordering of the seven excited states of 1,4-CHD. CASSCF overestimates the lowest excitation energy by about 2–3 eV, which makes the HOMO → LUMO excitation have higher energy than the other transitions. We may ascribe this failure to the limited correlation in a CASSCF calculation. In addition, MC-PDFT using ftPBE gives the smallest MUE (0.21 eV) for Rydberg excitation energies. When considering the valence and Rydberg excitation energies together, ftPBE is also found to be the best method in the table; it has a total MUE of 0.17 eV, slightly better than the 0.21 eV for tPBE.

In summary, Table 1 shows that MC-PDFT gives good excitation energies for both valence and Rydberg excited states for 1,4-CHD. Therefore we can explore the character of the states with more confidence than was possible in previous work.

3.2. Rydberg character analysis for 1,4-CHD

To explore the Rydberg or partial Rydberg character of each state for 1,4-CHD, we list the $\Delta\langle r^2\rangle$ values of each state based on

Table 1 The excitation energies (eV) calculated by CASSCF, CASPT2, XMS-CASPT2 and MC-PDFT and the experimental excitation energies (eV) for 1,4-CHD, together with the relative second moment (a_0^2) calculated from the corresponding CASSCF and CASPT2 wave functions for each state

State[a]	$\Delta\langle r^2\rangle_{(\text{CASSCF})}$	$\Delta\langle r^2\rangle_{(\text{CASPT2})}$	CASSCF	CASPT2	XMS-CASPT2	tPBE	ftPBE	Exp.
1,4-CHD (π-plus active space)								
$2^1A'$ (HOMO → LUMO)	19.3	19.3	8.26	7.01	7.14	5.76	5.83	5.80[c]
$1^1A''$(HOMO → 3s)	39.0	41.4	7.30	6.47	6.41	5.93	5.98	6.10[c,d]
$2^1A''$(HOMO → $3p_z$)	53.5	54.0	7.90	7.08	7.08	6.12	6.15	6.42[c,d]
$3^1A''$(HOMO → $3p_y$)[b]	45.7	46.7	7.46	6.77	7.89	6.31	6.33	N/A
$4^1A''$ (HOMO−1→ 3s)[b]	43.8	46.3	8.68	7.53	6.77	6.36	6.40	6.65[c,d]
$3^1A'$ (HOMO → $3p_x$)	32.5	30.9	7.67	7.50	7.60	6.56	6.59	N/A
$4^1A'$(HOMO−1→ LUMO)	24.4	24.1	9.28	8.25	8.31	6.80	6.88	7.05[c]
MUE (valence)			2.35	1.21	1.30	0.15	0.10	
MUE (Rydberg)			1.57	0.64	0.36	0.25	0.21	
MUE (all)			1.88	0.86	0.74	0.21	0.17	
1,4-CHD (π-only active space)								
$2^1A'$ (HOMO → LUMO)	11.2	10.9	8.00	6.59	6.71	5.19	5.20	5.80[c]
$4^1A'$(HOMO−1 → LUMO)	13.0	15.3	9.40	7.74	7.86	6.17	6.17	7.05[c]
MUE (valence)			2.28	0.74	0.86	0.75	0.74	

[a] The assignment of each state is according to CASSCF wave functions. [b] There is a mix between HOMO−1 → 3s and HOMO → $3p_y$ electron transition. The $3^1A''$ has 45.3% HOMO → $3p_y$ component and $4^1A''$ has 45.3% HOMO−1 → 3s component. [c] These results are obtained from the electron impact spectrum.[16] [d] These results are obtained from the optical spectrum,[17] as reassigned by Merchán *et al.*[15]

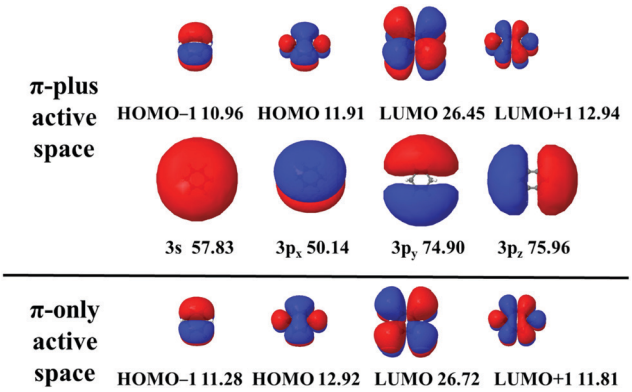

Fig. 2 The orbitals participating in the electronic excitation of 1,4-CHD and the corresponding second moments $\langle r^2 \rangle$ of each orbital based on the SA-CASSCF wave function obtained in π-plus active space. The value of the isodensity contour is 0.005 for each orbital. The orbitals are viewed from above the molecule, *i.e.*, in the *x* direction.

CASSCF wave functions and on CASPT2 first-order wave functions in Table 1. We find that there is no large difference between $\Delta\langle r^2 \rangle_{\mathrm{CASSCF}}$ and $\Delta\langle r^2 \rangle_{\mathrm{CASPT2}}$ for any of the states, which confirms that the CASSCF wave functions are quantitatively correct for the amount of diffuseness, even though their energies are not very accurate.

For valence excited states, we find that both the $2^1\mathrm{A}'$ and the $4^1\mathrm{A}'$ states have positive $\Delta\langle r^2 \rangle$ for either the π-only or the π-plus active space. Thus, even though these are valence excited states, they are more diffuse (have more Rydberg character) than the ground state. We also find that the state $\Delta\langle r^2 \rangle$ values calculated from the π-plus active space for the $2^1\mathrm{A}'$ and $4^1\mathrm{A}'$ states are increased compared to those calculated from the π-only active space. We think this is the reason why MC-PDFT gives better excitation energies in the π-plus active space – it is because that the π-plus active space gives a more accurate description of the partial Rydberg characters of the valence excited states.

For Rydberg excited states, we find – as expected – that they have even larger $\Delta\langle r^2 \rangle$ values than the valence excited states.

So far we have considered the moments of the states. We next try to understand the diffuse character by looking at the second moments of the orbitals that dominate the excitation processes. The orbital images and the second moments of these orbitals obtained from CASSCF wave functions for 1,4-CHD are summarized in Fig. 2 and Table 2.

We first consider the four π orbitals calculated from the π-plus active space. Fig. 2 shows that the LUMO orbital is more diffuse than HOMO and HOMO−1 orbitals. In Table 2, the $\langle x^2 \rangle$ of LUMO orbital is $7a_0^2$, while the $\langle x^2 \rangle$ for HOMO and HOMO−1 orbitals are only $\sim 3a_0^2$. The consequence is that the LUMO orbital has larger $\langle r^2 \rangle$ ($26a_0^2$) than the HOMO ($12a_0^2$) and HOMO−1 orbitals ($11a_0^2$), which confirms that the LUMO orbital is more diffuse. Since the first valence state $2^1\mathrm{A}'$ is produced by HOMO to LUMO excitation and the second valence state $4^1\mathrm{A}'$ is produced by HOMO−1 to LUMO excitation, this orbital analysis implies that these two valence excited states should have more Rydberg character than the ground state.

Table 2 The second moments $\langle x^2 \rangle$, $\langle y^2 \rangle$, $\langle z^2 \rangle$, and $\langle r^2 \rangle$ of the four π orbitals based on CASSCF wave functions for 1,4-CHD. The molecule is in the *yz* plane

Orbital	$\langle x^2 \rangle$ (a_0^2)	$\langle x^2 \rangle$ (a_0^2)	$\langle z^2 \rangle$ (a_0^2)	$\langle r^2 \rangle$ (a_0^2)
HOMO−1[a]	2.26/2.42	6.76/6.89	1.94/1.97	10.96/11.28
HOMO[a]	2.43/2.61	5.76/5.37	3.71/4.93	11.91/12.92
LUMO[a]	6.95/7.05	11.06/11.03	8.44/8.64	26.45/26.72
LUMO+1[a]	2.11/1.83	6.21/5.98	4.62/4.00	12.94/11.81
3s	10.82	23.47	23.54	57.83
3p$_x$	28.27	9.92	11.95	50.14
3p$_y$	11.88	46.89	16.12	74.90
3p$_z$	13.87	15.14	46.95	75.96

[a] The value before the solidus is calculated from π-plus active space, and the value after the solidus is calculated from π-only active space.

We then compare the four π orbitals calculated from the π-plus and π-only active spaces. Table 2 shows that even though the $\langle r^2 \rangle$ of the LUMO orbital calculated from the π-plus active space does not change much compared to that calculated from the π-only active space, the $\langle r^2 \rangle$ of the HOMO orbital is decreased to $11.9a_0^2$ from $12.9a_0^2$, and the $\langle r^2 \rangle$ of the HOMO−1 orbital is decreased to $11.0a_0^2$ from $11.3a_0^2$. This explains why the state $\Delta\langle r^2 \rangle$ values calculated from the π-plus active space for the $2^1\mathrm{A}'$ and $4^1\mathrm{A}'$ states are increased compared to those calculated from the π-only active space and further confirms that the π-plus active space gives a more accurate description of the partial Rydberg character for valence excited states.

We finally consider the Rydberg orbitals that can only be obtained in the π-plus active space. Table S3 (ESI†) identifies excited orbital in the dominant configuration of each state. For example, the dominant excited orbitals of the $2^1\mathrm{A}''$, $3^1\mathrm{A}''$, $3^1\mathrm{A}'$, $1^1\mathrm{A}''$, and $4^1\mathrm{A}''$ states are the 3p$_z$, 3p$_y$, and 3p$_x$, 3s, and 3s orbitals, respectively. Looking at the second moments of orbitals in Table 2, we find that all the Rydberg orbitals have larger $\langle r^2 \rangle$ (larger than $50a_0^2$) than the LUMO orbital (for which $\langle r^2 \rangle$ is $26a_0^2$). This is consistent with the result that the Rydberg excited states, for which $\Delta\langle r^2 \rangle$ ranges from 33 to $54a_0^2$, are more diffuse than the valence excited states, for which $\Delta\langle r^2 \rangle$ is around $22a_0^2$. We conclude that the analysis of the orbital moments confirms the conclusions from the analysis of the state moments about the Rydberg character that the π-plus active space yields for all the low-lying states of 1,4-CHD.

3.3. Excitation energies of 1,3-CHD

The excitation energies obtained by CASSCF, CASPT2, XMS-CASPT2, and MC-PDFT for 1,3-CHD are summarized in Table 3. We must use the π-plus active space to get all the states (the π-only active space yields only the valence states), but the table shows that the π-plus active space increases the error for CASPT2 and XMS-CASPT2, showing the difficulty of treating the whole set of states consistently by perturbation theory. However, MC-PDFT with either on-top functional provides good results for both valence and Rydberg states with an overall MUE of only 0.23 eV for tPBE and 0.25 eV for ftPBE. Furthermore, unlike the more expensive CASPT2 and XMS-CASPT2, MC-PDFT gives the correct energy ordering for all six excited states for which experimental data are available, except that the order of

Table 3 The excitation energies (eV) calculated by CASSCF, CASPT2, XMS-CASPT2, and MC-PDFT and the experimental excitation energies (eV) for 1,3-CHD, together with the relative second moment (a_0^2) calculated from the corresponding CASSCF and CASPT2 wave functions for each state

State[a]	$\Delta\langle r^2\rangle_{(CASSCF)}$	$\Delta\langle r^2\rangle_{(CASPT2)}$	CASSCF	CASPT2	XMS-CASPT2	tPBE	ftPBE	Exp.[b]
1,3-CHD (π-plus active space)								
1^1B (HOMO → LUMO)	11.9	14.8	8.16	6.03	6.51	5.06	5.11	4.94
2^1A (HOMO → 3s)	41.0	39.9	5.33	5.96	6.83	5.30	5.40	5.39[c]
2^1B (HOMO → $3p_y$)	51.5	50.9	6.57	6.37	5.01	5.83	5.91	6.03[c]
3^1B (HOMO → $3p_x$)	41.4	41.3	6.84	6.53	6.30	5.94	6.01	N/A
3^1A (HOMO → $3p_z$)	54.4	53.0	5.92	6.58	6.18	5.75	5.85	6.05[c]
4^1A (mixed valence state)	24.6	24.9	6.30	6.57	7.34	5.95	5.97	6.30
MUE (valence)			1.61	0.68	1.31	0.23	0.25	0.17
MUE (Rydberg)			0.24	0.48	0.86	0.20	0.11	
MUE (all)			0.79	0.56	1.04	0.21	0.17	
1,3-CHD (π-only active space)								
1^1B (HOMO → LUMO)	8.1	8.2	7.01	5.25	5.25	3.75	3.85	4.94
4^1A (mixed valence state)	1.7	1.6	6.47	6.50	6.63	6.56	6.48	6.30
MUE (valence)			1.12	0.26	0.32	0.73	0.64	

[a] The assignment of each state is according to CASSCF wave functions. [b] The results are obtained from the electron impact spectroscopy,[18] optical spectra,[20,21] and electron energy loss spectra.[19] [c] The results are obtained from the optical and resonance-enhanced multiphoton ionization spectra.[15]

3^1A and 2^1B (which differ by only 0.02 eV) is switched. These results further validate MC-PDFT for calculating both the valence and Rydberg excitation energies and prove that the π-plus active space is sufficient to obtain accurate results for all the low-lying states.

3.4. Rydberg character analysis for 1,3-CHD

We list the $\Delta\langle r^2\rangle$ value of each state calculated based on CASSCF wave functions and CASPT2 first-order wave functions in Table 3 to understand the Rydberg character of each state. As for 1,4-CHD, we again find that there is no large difference between $\Delta\langle r^2\rangle_{CASSCF}$ and $\Delta\langle r^2\rangle_{CASPT2}$ for all the states, which is very encouraging since MC-PDFT is based on the CASSCF density.

Table 3 shows that (as expected) the valence excited states have larger $\langle r^2\rangle$ than the ground state, and the Rydberg excited states have even larger $\langle r^2\rangle$ than the valence excited states. These results for the moments of the states can be explained by the orbital images in Fig. 3 and the second moments of the orbitals in Table 4. In particular, we find that both the LUMO and the LUMO+1 orbitals have larger $\langle r^2\rangle$ than the HOMO and HOMO−1 orbitals, and all the Rydberg orbitals have larger $\langle r^2\rangle$ than all the four valence π orbitals.

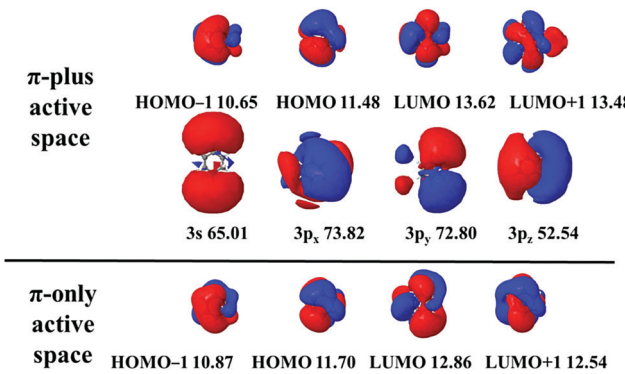

Fig. 3 The orbitals participating in the electronic excitation of 1,3-CHD and the corresponding second moments $\langle r^2\rangle$ of each orbital based on the SA-CASSCF wave function obtained in π-plus active space. The value of the isodensity contour is 0.005 for each orbital. The orbitals are viewed from above the molecule, *i.e.*, in the *x* direction.

Table 4 The second moments $\langle x^2\rangle$, $\langle y^2\rangle$, $\langle z^2\rangle$, and $\langle r^2\rangle$ of the orbitals based on CASSCF wave functions for 1,3-CHD. The molecule is in the *yz* plane

Orbital	$\langle x^2\rangle$ (a_0^2)	$\langle y^2\rangle$ (a_0^2)	$\langle z^2\rangle$ (a_0^2)	$\langle r^2\rangle$ (a_0^2)
HOMO−1[a]	2.35/2.37	3.80/3.54	4.51/4.96	10.65/10.87
HOMO[a]	2.36/2.44	6.57/6.89	2.55/2.37	11.48/11.70
LUMO[a]	2.63/2.35	6.90/7.16	4.09/3.34	13.62/12.86
LUMO+1[a]	2.42/2.08	5.34/4.97	5.73/5.48	13.48/12.54
3s	16.68	13.85	34.48	65.01
$3p_x$	28.48	17.45	27.89	73.82
$3p_y$	12.54	43.09	17.17	72.80
$3p_z$	22.12	8.98	21.44	52.54

[a] The value before the solidus is calculated from π-plus active space, and the value after the solidus is calculated from π-only active space.

Even though the 1,4-CHD (unconjugated) and 1,3-CHD (conjugated) molecules have many similar features in terms of the Rydberg character of the orbitals, they still have some significant differences. For example, the diffuseness of the LUMO orbitals is different in the two molecules. In the unconjugated case, the $\langle r^2\rangle$ values of HOMO, HOMO−1, and LUMO+1 orbitals are in the 10 to 14a_0^2 range, while the LUMO orbital has a much larger $\langle r^2\rangle$ (26a_0^2). In the conjugated case, on the contrary, all the four π orbitals have the same amount of diffuseness in that their $\langle r^2\rangle$ are all in the range from 10 to 14a_0^2.

4. Conclusions

We have used CASSCF, CASPT2, XMS-CASPT2, and MC-PDFT to compute the excitation energies of both valence states and Rydberg states for two dienes: 1,4-CHD and 1,3-CHD. Two sets of active space, one with only valence orbitals (π-only active space) and the other also containing Rydberg orbitals (π-plus active space), are tested for the two molecules. The results show

that the π-plus active space gives better excitation energies in MC-PDFT calculations and a different description of the partial Rydberg character of the valence excited states. Thus, we conclude that, consistent with the ''Goldilocks principle'' for choosing basis sets,[36] Rydberg orbitals should be included in the active space to calculate the excitation energy for dienes.

The MC-PDFT results demonstrate that the two on-top functionals, ftPBE and tPBE, give the best approximations of the excitation energies when the density is represented by the optimized CASSCF wave function using an active space containing diffuse orbitals. Furthermore, the moment analysis of the CASSCF states and CASPT2 states shows that the character of the orbitals is not changed significantly by external correlation (dynamic correlation outside the active space), even though the energies are greatly changed. This is very encouraging because it indicates that the accuracy of the MC-PDFT energies does not suffer from having poor densities at the CASSCF level. The accurate energies obtained with MC-PDFT are also very encouraging because of the low computational cost of MC-PDFT, which has a similar cost to CASSCF and so is more affordable than CASPT2 or XMS-CASPT2 for more complex dienes.

A special characteristic of the present analysis is the calculation of the second moments of the excited-state orbitals. Since the CASPT2 densities agree well with the CASSCF ones and since the MC-PDFT methods get accurate excitation energies based on the CASSCF densities, we believe that we can trust these moments as far as giving a more accurate picture of the diffuseness of the excited state orbitals in these prototype molecules than has previously been available.

Conflicts of interest

There are no conflicts to declare.

Acknowledgements

The authors are grateful to Laura Gagliardi for many helpful discussions. This work was supported in part by the National Science Foundation under grant CHE–1746186.

References

1 M. Irie, Diarylethenes for memories and switches, *Chem. Rev.*, 2000, **100**, 1685–1716.
2 K. L. Kompa and R. D. Levine, A molecular logic gate, *Proc. Natl. Acad. Sci. U. S. A.*, 2001, **98**, 410–414.
3 M. A. Wolak, N. B. Gillespie, C. J. Thomas, R. R. Birge and W. J. Lees, Optical properties of photochromic fluorinated indolylfulgides, *J. Photochem. Photobiol., A*, 2001, **144**, 83–91.
4 E. Havinga and J. L. M. A. Schlatmann, Remarks on the specificities of the photochemical and thermal transformations in the vitamin D field, *Tetrahedron*, 1961, **16**, 146–152.
5 N. A. Anderson, J. J. Shiang and R. J. Sension, Subpicosecond ring opening of 7-dehydrocholesterol studied by ultrafast spectroscopy, *J. Phys. Chem. A*, 1999, **103**, 10730–10736.
6 J. Meyer-Ilse, D. Akimov and B. Dietzek, Ultrafast circular dichroism study of the ring opening of 7-dehydrocholesterol, *J. Phys. Chem. Lett.*, 2012, **3**, 182–185.
7 E. Havinga, R. J. de Kock and M. P. Rappoldt, The photochemical interconversions of provitamin D, lumisterol, previtamin D and tachysterol, *Tetrahedron*, 1960, **11**, 276–284.
8 W. G. Dauben, P. E. Share and R. R. Ollmann, Triene photophysics and photochemistry: previtamin D3, *J. Am. Chem. Soc.*, 2002, **110**, 2548–2554.
9 (*a*) S. Deb and P. M. Weber, The Ultrafast Pathway of Photon-Induced Electrocyclic Ring-Opening Reactions: The Case of 1,3-Cyclohexadiene, *Annu. Rev. Phys. Chem.*, 2011, **62**, 19–39; (*b*) O. Schalk, A. E. Boguslavskiy, A. Stolow and M. S. Schuurman, Through-Bond Interactions and the Localization of Excited-State Dynamics, *J. Am. Chem. Soc.*, 2011, **133**, 16451–16458; (*c*) J. L. White, J. Kim, V. S. Petrovi and P. H. Bucksbaum, Ultrafast ring opening in 1,3-cyclohexadiene investigated by simplex-based spectral unmixing, *J. Chem. Phys.*, 2012, **136**, 054303; (*d*) B. C. Arruda and R. J. Sension, Ultrafast polyene dynamics: The ring opening of 1,3-cyclohexadiene derivatives, *Phys. Chem. Chem. Phys.*, 2014, **16**, 4439–4455; (*e*) C. C. Pemberton, Y. Zhang, K. Saita, A. Kirrander and P. M. Weber, From the (1B) Spectroscopic State to the Photochemical Product of the Ultrafast Ring-Opening of 1,3-Cyclohexadiene: A Spectral Observation of the Complete Reaction Path, *J. Phys. Chem. A*, 2015, **119**, 8832–8845; (*f*) C. C. Pemberton, Y. Zhang, K. Saita, A. Kirrander and P. M. Weber, From the (1B) Spectroscopic State to the Photochemical Product of the Ultrafast Ring-Opening of 1,3-Cyclohexadiene: A Spectral Observation of the Complete Reaction Path, *J. Phys. Chem. A*, 2015, **119**, 8832–8845; (*g*) O. Schalk, T. Geng, T. Thompson, N. Baluyot, R. D. Thomas, E. Tapavicza and T. Hansson, Cyclohexadiene Revisited: A Time-Resolved Photoelectron Spectroscopy and ab Initio Study, *J. Phys. Chem. A*, 2016, **120**, 2320–2329; (*h*) M. Tudorovskaya, R. S. Minns and A. Kirrander, Effects of probe energy and competing pathways on time-resolved photoelectron spectroscopy: The ring-opening of 1,3-cyclohexadiene, *Phys. Chem. Chem. Phys.*, 2018, **20**, 17714–17726; (*i*) I. Polyak, L. Hutton, R. Crespo-Otero, M. Barbatti and P. J. Knowles, Ultrafast Photoinduced Dynamics of 1,3-Cyclohexadiene Using XMS-CASPT2 Surface Hopping, *J. Chem. Theory Comput.*, 2019, **15**, 3929–3940.
10 M. H. Kibel, M. K. Livett and G. L. Nyberg, Angular distribution photoelectron spectroscopic assignment of π-orbital states in 1,4-cyclohexadiene, *J. Electron Spectrosc. Relat. Phenom.*, 1978, **14**, 155–157.
11 E. Heilbronner, F. Brogli and E. Vogel, Photoelectron spectroscopic assignment of symmetry to the ground state and first excited state of the 1,4-cyclohexadiene radical cation, *J. Electron Spectrosc. Relat. Phenom.*, 1976, **9**, 227–239.
12 E. Heilbronner and A. Schmelzer, A Quantitative Assessment of ''Through-space'' and ''Through-bond'' Interactions. Application to Semi-empirical SCF Models, *Helv. Chim. Acta*, 1975, **58**, 936–967.
13 R. Hoffmann, E. Heilbronner and R. Gleiter, Interaction of nonconjugated double bonds, *J. Am. Chem. Soc.*, 2002, **92**, 706–707.

14 R. Hoffmann, Interaction of orbitals through space and through bonds, *Acc. Chem. Res.*, 2002, **4**, 1–9.
15 M. Merchán, L. Serrano-Andrés, L. S. Slater, B. O. Roos, R. McDiarmid and X. Xing, Electronic Spectra of 1,4-Cyclohexadiene and 1,3-Cyclohexadiene: A Combined Experimental and Theoretical Investigation, *J. Phys. Chem. A*, 1999, **103**, 5468–5476.
16 R. McDiarmid and J. P. Doering, Electron impact investigation of the electronic transitions of 1,4-cyclohexadiene and 1,5-cyclooctadiene, *J. Chem. Phys.*, 1981, **75**, 2687–2692.
17 D. A. Demeo and A. J. Yencra, Photoelectron spectra of bicyclic and exocyclic olefins, *J. Chem. Phys.*, 1970, **53**, 4536–4543.
18 R. P. Frueholz, W. M. Flicker, O. A. Mosher and A. Kuppermann, Excited electronic states of cyclohexene, 1,4-cyclohexadiene, norbornene, and norbornadiene as studied by electron-impact spectroscopy, *J. Chem. Phys.*, 1979, **70**, 1986–1993.
19 R. McDiarmid, A. Sabljić and J. P. Doering, Valence transitions in 1,3-cyclopentadiene, 1,3-cyclohexadiene, and 1,3-cycloheptadiene, *J. Chem. Phys.*, 1985, **83**, 2147–2152.
20 M. B. Robin, *Higher excited states of polyatomic molecules*, Academic Press, New York, 1975, vol. II.
21 B. L. Sowers, E. T. Arakawa and R. D. Birkhoff, Optical properties of six-member carbon ring organic liquids in the vacuum ultraviolet, *J. Chem. Phys.*, 1971, **54**, 2319–2324.
22 N. Kuthirummal, F. M. Rudakov, C. L. Evans and P. M. Weber, Spectroscopy and femtosecond dynamics of the ring opening reaction of 1,3-cyclohexadiene, *J. Chem. Phys.*, 2006, **13**, 133307.
23 W. Cheng, C. L. Evans, N. Kuthirummal and P. M. Weber, A 9 eV superexcited state of 1,3-cyclohexadiene revealed by double resonance ionization photoelectron spectroscopy, *Chem. Phys. Lett.*, 2001, **349**, 405–410.
24 J. L. White, J. Kim, V. S. Petrovi and P. H. Bucksbaum, Ultrafast ring opening in 1,3-cyclohexadiene investigated by simplex-based spectral unmixing, *J. Chem. Phys.*, 2012, **5**, 054303.
25 R. C. Dudek and P. M. Weber, Ultrafast diffraction imaging of the electrocyclic ring-opening reaction of 1,3-cyclohexadiene, *J. Phys. Chem. A*, 2001, **105**, 4167–4171.
26 S. Adachi, M. Sato and T. Suzuki, Direct observation of ground-state product formation in a 1,3-cyclohexadiene ring-opening reaction, *J. Phys. Chem. Lett.*, 2015, **6**, 343–346.
27 W. Fuß, W. E. Schmid and S. A. Trushin, Time-resolved dissociative intense-laser field ionization for probing dynamics: Femtosecond photochemical ring opening of 1,3-cyclohexadiene, *J. Chem. Phys.*, 2000, **112**, 8347–8362.
28 S. A. Trushin, W. Fuß, T. Schikarski, W. E. Schmid and K. L. Kompa, Femtosecond photochemical ring opening of 1,3-cyclohexadiene studied by time-resolved intense-field ionization, *J. Chem. Phys.*, 1997, **106**, 9386–9389.
29 K. Kosma, S. A. Trushin, W. Fuß and W. E. Schmid, Cyclohexadiene ring opening observed with 13 fs resolution: Coherent oscillations confirm the reaction path, *Phys. Chem. Chem. Phys.*, 2009, **11**, 172–181.
30 W. Fuß, T. Schikarski, W. E. Schmid, S. Trushin and K. L. Kompa, Ultrafast dynamics of the photochemical ring opening of 1,3-cyclohexadiene studied by multiphoton ionization, *Chem. Phys. Lett.*, 1996, **262**, 675–682.
31 S. Pullen, L. A. Walker, B. Donovan and R. J. Sension, Femtosecond transient absorption study of the ring-opening reaction of 1,3-cyclohexadiene, *Chem. Phys. Lett.*, 1995, **242**, 415–420.
32 H. Tamura, S. Nanbu, H. Nakamura and T. Ishida, A theoretical study of cyclohexadiene/hexatriene photochemical interconversion: Multireference configuration interaction potential energy surfaces and transition probabilities for the radiationless decays, *Chem. Phys. Lett.*, 2005, **401**, 487–491.
33 C. C. Pemberton, Y. Zhang, K. Saita, A. Kirrander and P. M. Weber, From the (1B) spectroscopic state to the photochemical product of the ultrafast ring-opening of 1,3-cyclohexadiene: a spectral observation of the complete reaction path, *J. Phys. Chem. A*, 2015, **119**, 8832–8845.
34 Y. Lei, H. Wu, X. Zheng, G. Zhai and C. Zhu, Photo-induced 1,3-cyclohexadiene ring opening reaction: Ab initio on-the-fly nonadiabatic molecular dynamics simulation, *J. Photochem. Photobiol., A*, 2016, **317**, 39–49.
35 I. Polyak, L. Hutton, R. Crespo-Otero, M. Barbatti and P. J. Knowles, Ultrafast photoinduced dynamics of 1,3-cyclohexadiene using XMS-CASPT2 surface hopping, *J. Chem. Theory Comput.*, 2019, **15**, 3929–3940.
36 S. S. Dong, L. Gagliardi, D. G. Truhlar and D. G. Truhlar, Nature of the 1^1B_u and 2^1A_g excited states of butadiene and the Goldilocks principle of basis set diffuseness, *J. Chem. Theory Comput.*, 2019, **15**, 4591–4601.
37 B. O. Roos, P. R. Taylor and P. E. M. Sigbahn, A complete active space SCF method (CASSCF) using a density matrix formulated super-CI approach, *Chem. Phys.*, 1980, **48**, 157–173.
38 B. O. Roos, P. Linse, P. E. M. Siegbahn and M. R. A. Blomberg, A simple method for the evaluation of the second-order-perturbation energy from external double-excitations with a CASSCF reference wavefunction, *Chem. Phys.*, 1982, **66**, 197–207.
39 K. Andersson, P. Å. Malmqvist and B. O. Roos, Second-order perturbation theory with a complete active space self-consistent field reference function, *J. Chem. Phys.*, 1992, **96**, 1218–1226.
40 K. Andersson, P. Aake. Malmqvist, B. O. Roos, A. J. Sadlej and K. Wolinski, Second-order perturbation theory with a CASSCF reference function, *J. Phys. Chem.*, 2002, **94**, 5483–5488.
41 P. Celani and H. J. Werner, Multireference perturbation theory for large restricted and selected active space reference wave functions, *J. Chem. Phys.*, 2000, **112**, 5546–5557.
42 T. Shiozaki and H. J. Werner, Communication: Second-order multireference perturbation theory with explicit correlation: CASPT2-F12, *J. Chem. Phys.*, 2010, **133**, 141103.
43 T. Shiozaki, W. Gyroffy, P. Celani and H. J. Werner, Communication: Extended multi-state complete active space second-order perturbation theory: Energy and nuclear gradients, *J. Chem. Phys.*, 2011, **135**, 081106.
44 A. A. Granovsky, Extended multi-configuration quasi-degenerate perturbation theory: The new approach to multi-state multi-reference perturbation theory, *J. Chem. Phys.*, 2011, **134**, 214113.

45 G. Li Manni, R. K. Carlson, S. Luo, D. Ma, J. Olsen, D. G. Truhlar and L. Gagliardi, Multiconfiguration pair-density functional theory, *J. Chem. Theory Comput.*, 2014, **10**, 3669–3680.
46 E. Papajak, H. R. Leverentz, J. Zheng and D. G. Truhlar, Efficient diffuse basis sets: cc-pV*x*Z+ and maug-cc-pV*x*Z, *J. Chem. Theory Comput.*, 2009, **5**, 1197–1202.
47 T. H. Dunning, Gaussian basis sets for use in correlated molecular calculations. I. The atoms boron through neon and hydrogen, *J. Chem. Phys.*, 1989, **90**, 1007–1023.
48 R. A. Kendall, T. H. Dunning and R. J. Harrison, Electron affinities of the first-row atoms revisited. Systematic basis sets and wave functions, *J. Chem. Phys.*, 1992, **96**, 6796–6806.
49 S. Vancoillie, M. G. Delcey, R. Lindh, V. Vysotskiy, P. Å. Malmqvist and V. Veryazov, Parallelization of a multiconfigurational perturbation theory, *J. Comput. Chem.*, 2013, **34**, 1937–1948.
50 F. Aquilante, J. Autschbach, R. K. Carlson, L. F. Chibotaru, M. G. Delcey, L. De Vico, I. Fdez. Galván, N. Ferré, L. M. Frutos, L. Gagliardi, M. Garavelli, A. Giussani, C. E. Hoyer, G. Li Manni, H. Lischka, D. Ma, P. Å. Malmqvist, T. Müller, A. Nenov, M. Olivucci, T. B. Pedersen, D. Peng, F. Plasser, B. Pritchard, M. Reiher, I. Rivalta, I. Schapiro, J. Segarra-Martí, M. Stenrup, D. G. Truhlar, L. Ungur, A. Valentini, S. Vancoillie, V. Veryazov, V. P. Vysotskiy, O. Weingart, F. Zapata and R. Lindh, Molcas 8: New capabilities for multiconfigurational quantum chemical calculations across the periodic table, *J. Comput. Chem.*, 2016, **37**, 506–541.
51 W. Kohn and L. J. Sham, Self-consistent equations including exchange and correlation effects, *Phys. Rev.*, 1965, **140**, A1133.
52 Y. Zhao and D. G. Truhlar, The M06 suite of density functionals for main group thermochemistry, thermochemical kinetics, noncovalent interactions, excited states, and transition elements: Two new functionals and systematic testing of four M06-class functionals and 12 other functionals, *Theor. Chem. Acc.*, 2008, **120**, 215–241.
53 H. Oberhammer and S. H. Bauer, Structures and conformations of the cyclohexadienes, *J. Am. Chem. Soc.*, 1969, **91**, 10–16.
54 G. Ghigo, B. O. Roos and P. Å. Malmqvist, A modified definition of the zeroth-order Hamiltonian in multiconfigurational perturbation theory (CASPT2), *Chem. Phys. Lett.*, 2004, **396**, 142–149.
55 B. O. Roos and K. Andersson, Multiconfigurational perturbation theory with level shift - the Cr_2 potential revisited, *Chem. Phys. Lett.*, 1995, **245**, 215–223.
56 B. O. Roos, K. Andersson, M. P. Fülscher, L. Serrano-Andrés, K. Pierloot, M. Merchán and V. Molina, Applications of level shift corrected perturbation theory in electronic spectroscopy, *THEOCHEM*, 1996, **388**, 257–276.
57 J. P. Perdew, K. Burke and M. Ernzerhof, Generalized gradient approximation made simple, *Phys. Rev. Lett.*, 1996, **77**, 3865–3868.
58 R. K. Carlson, D. G. Truhlar and L. Gagliardi, Multiconfiguration pair-density functional theory: A fully translated gradient approximation and its performance for transition metal dimers and the spectroscopy of $Re_2Cl_8^{2-}$, *J. Chem. Theory Comput.*, 2015, **11**, 4077–4085.
59 D. E. Love, D. Nachtigallova, K. D. Jordan, J. M. Lawson and M. N. Paddon-Row, Electronically Excited States of 1,4:5,8-Bismethano-1,4,4a,5,8,8a-hexahydronaphthalene, a Nonconjugated Diene: Comparison of Theory and Experiment, *J. Am. Chem. Soc.*, 1996, **118**, 1235–1240.